



Review

Mechanical and Magnetic Properties of the High-Entropy Alloys for Combinatorial Approaches

E-Wen Huang ^{1,2,*}, Guo-Yu Hung ¹, Soo Yeol Lee ³, Jayant Jain ⁴, Kuan-Pang Chang ¹,
Jing Jhe Chou ¹, Wen-Chi Yang ¹ and Peter K. Liaw ⁵

¹ Department of Materials Science & Engineering, National Chiao Tung University, Hsinchu 30010, Taiwan; bigegg123@gmail.com (G.-Y.H.); 9901eric@gmail.com (K.-P.C.); energy106@gmail.com (J.J.C.); zxc3110412@gmail.com (W.-C.Y.)

² Department of Materials Science & Engineering, National Chiao Tung University, Hsinchu 30013, Taiwan

³ Department of Materials Science and Engineering, Chungnam National University, Daejeon 34134, Korea; sylee2012@cnu.ac.kr

⁴ Department of Materials Science and Engineering, Indian Institute of Technology, New Delhi 110016, India; jayantj@am.iitd.ac.in

⁵ Department of Materials Science & Engineering, University of Tennessee, Knoxville, TN 37996-2100, USA; pliaw@utk.edu

* Correspondence: ewhuang@g2.nctu.edu.tw

Received: 19 February 2020; Accepted: 5 March 2020; Published: 14 March 2020



Abstract: This review summarizes the state of high-entropy alloys and their combinatorial approaches, mainly considering their magnetic applications. Several earlier studies on high-entropy alloy properties, such as magnetic, wear, and corrosion behavior; different forms, such as thin films, nanowires, thermal spray coatings; specific treatments, such as plasma spraying and inclusion effects; and unique applications, such as welding, are summarized. High-entropy alloy systems that were reported for both their mechanical and magnetic properties are compared through the combination of their Young's modulus, yield strength, remanent induction, and coercive force. Several potential applications requiring both mechanical and magnetic properties are reported.

Keywords: high-entropy alloys; complex concentrated alloys; mechanical behavior; magnetic properties

1. Introduction

In 2004, Professor Jien-Wei Yeh reported the concept of high-entropy alloys, which are beyond traditional principal-element alloys, with multiple principal elements [1], and Professor Brian Cantor presented the development of equiatomic multicomponent alloys [2]. The results of both investigators created a new direction for the exploration in metallurgy, which is not conventionally categorized by principal elements. For the past fifteen years, high-entropy alloys with potential use for various applications in different groups of metal elements have been developed. In 2016, Miracle and Senkov categorized high-entropy alloys, multi-principal-element alloys (MPEAs), and equiatomic multicomponent alloys in terms of complex, concentrated alloys (CCAs) [3]. Diao *et al.* also call them metal buffets [4].

The mechanical properties of different families of high-entropy alloys extend the limits of possible operating-environment temperatures of metallic systems to cryogenic [5] and elevated temperatures [6,7]. These large groups of high-entropy alloys possess several fundamental properties, such as those for the cocktail effects. Moreover, the mechanical metallurgy characteristics of these high-entropy alloys are needed for their systematic development. Starting from basic metallurgical principles, Jones and Ashby have summarized the microstructure-insensitive properties of high-entropy

alloys, such as their densities, moduli, coefficients of thermal expansion, and specific heats [8]. Microstructure-sensitive properties include yield and tensile strengths, ductility, fracture toughness, and creep and fatigue strength [8]. These properties depend on the heat treatment, mechanical metallurgy, and the specific alloy compositions. For steels, these investigators have concluded that even when the composition is nearly identical, these microstructure-sensitive properties may yet vary, subject to the history of the heat and mechanical treatments of the metallic system [8]. For high-entropy alloys, microstructure-sensitive behavior can be much more complicated. Moreover, Ding et al. showed that the element-dependent local arrangement of the high-entropy alloys, such as staggered positive and negative strain fields at nanoscale, can change the mechanical properties significantly [9]. The composition–structure–property relationships seem infinite for the design of high-entropy alloys [3,10].

With innovations in manufacturing [11,12], characterization [13–16], high-throughput examinations [17,18], and computation technology [19–22], the aforementioned complexity seems to become solvable puzzles for materials scientists [23,24]. Systematic investigations into the high-entropy enhancement and interplay with microstructure-sensitive and -insensitive properties are expected to yield combinatorial approaches for functional applications, such as for superconductivity [25], catalysts [26], and magnetics [27,28]. As shown in Borkar et al.'s work [29], it is important to consider the combinatorial approaches, especially for mechanical and magnetic properties. This article reviews the history and advances of high-entropy alloys for future high-throughput combinatorial approaches, with a focus on the mechanical and magnetic behavior.

2. History of High-Entropy Alloys for Combinatorial Approaches

High-entropy alloys are well-known as structural materials for their excellent mechanical properties [3]. Exceptional mechanical properties have been reported for the Cantor alloys [5], dual-phase high-entropy alloys [30], and intermetallics-strengthened high-entropy alloys [31]. For comparison of the mechanical properties of high-entropy alloys relative to the conventional alloys, Figure 1 presents the yield strength and Young's moduli of a few selected representative metals and several high-entropy alloys.

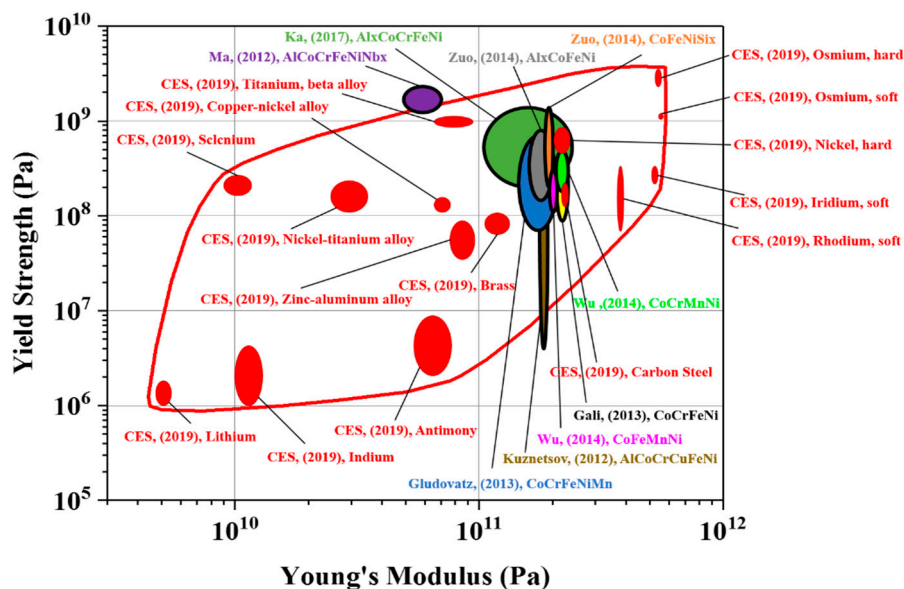


Figure 1. Yield strength ($\sigma_{0.2}$) of several conventional alloys, including stainless steel, aluminum, titanium, and nickel-based alloys and high-entropy alloys. (Data taken from [5,32–44]). The data is from the CES EduPack 2009, Granta Design, Limited, Cambridge, UK, 2009.

With regard to applications of high-entropy alloys, Zhang et al. commented that the combination of functional properties, such as magnetic and electric, as well as mechanical performance, such as

yield strength and elongation, makes high-entropy alloys excellent soft magnetic materials (SMM) [27]. High-entropy alloy (HEA)-based functional materials are thus advantageous for their excellent mechanical properties for endurance [10].

Even before the first two high-entropy alloys published in 2004 [1,2], Professor Yeh and several other teams had already focused on combinatorial approaches for the high-entropy-alloy research and development, as listed in Table 1, which chronically summarizes the early research into high-entropy-alloy combinatorial approaches through 2004. These results are mainly archived from different groups' dissertations and theses. Several potential applications and research areas have been explored. These applications range from thin films [45–48], magnetic behavior [47], nanowires [49], thermal spray coatings [50,51], plasma spraying [52], corrosion behavior [53,54], welding [55], inclusion effects [56], and wear properties [57,58]. The latest magnetic applications of high-entropy alloys are summarized in the later sections of this manuscript.

Table 1. Summary of research into high-entropy alloy (HEA) combinatorial approaches from 1996 to 2004.

Title	Year	HEA System	Reference	Thesis Type
A study on the Multicomponent Alloy Systems Containing Equal-Mole Elements	1996	Al-Ti-V-Cr-Fe-Co-Ni-Cu-Zr-Mo-Pd	[59]	Master
Properties of the Multicomponent Alloy System with Equal-Mole Elements	1998		[60]	Master
A Study on the Multicomponent Alloy Systems with Equal-Mole Face-Centered Cubic (FCC) or Body-Centered Cubic (BCC) Elements	2000	Ni-Co-Fe-Cu-V-Cr-Mo-Au-Ag-Ti-Al-Zr-Y-Nd	[61]	Master
A Study on the Cu-Ni-Al-Co-Cr-Fe-Si-Ti Multicomponent Alloy System	2001	Cu-Ni-Al-Co-Cr-Fe-Si-Ti	[62]	Master
Development of Multicomponent High-Entropy Alloys for Thermal Spray Coating	2002	Fe-Ni-Co-Cr-Si	[50]	Master
NiAlFeCuCoCr-6-Component Alloy Metal Films Structure	2002	Ni-Al-Fe-Cu-Co-Cr	[45]	Master
Study on the Corrosion Behavior and Thin Film Properties of Cr-Fe-Co-Ni-Cu-Al _x High-Entropy Alloys	2003	Cr-Fe-Co-Ni-Cu-Al _x	[53]	Master
Research of Multi-component High-Entropy Alloys for Thermal Spray Coating	2003	Mo _{0.5} (Al-Si-Ti-Cr-Fe-Co-Ni-Mo) _{0.5} and Mo _{0.5} (Al-Si-Ti-Cr-Fe-Ni-Mo) _{0.5} Zr _x (Al-Si-Ti-Cr-Fe-Ni-Zr) _{1-x}	[51]	Master
The Effect of V, Si, Ti Addition on the Microstructure and Wear Properties of Al(0.5)CrCuFeCoNi High-Entropy Alloys	2003	Al _{0.5} Cr-Cu-Fe-Co-Ni	[57]	Master
Study on the Microstructure and Electrical Properties Evolution of High-Entropy Alloy Thin Films	2003	Cu _{0.5} Ni-Al-Co-Cr-Fe-Ti	[46]	Master
Development on the High Frequency Soft-Magnetic Thin Films from High-Entropy Alloys	2003	Fe ₄₂ Co ₃₇ Ni ₁₀ Al ₅ B ₆ and Fe ₄₀ Co ₃₅ Al ₅ Ni ₅ Cr ₅ Si ₁₀	[47]	Master
Research on the Bulks and Thin Film Properties of CrMoNbTiZr High-entropy alloys	2004	Cr-Mo-Nb-Ti-Zr	[48]	Master
Corrosion Behavior of FeCoNiCrCu _x High-Entropy Alloys in Various Aqueous Solutions	2004	Fe-Co-Ni-Cr-Cu _x	[54]	Master
The Study of Different Welding with High-Entropy and SUS304 Stainless Steels	2004		[55]	Master

Table 1. Cont.

Title	Year	HEA System	Reference	Thesis Type
Investigation of the Machinability of Five Kinds of High-Entropy Alloys and the Effects of Al, Cu, Co Elements Inclusion	2004	Fe ₁ Co ₁ Ni ₁ Cr ₁ Cu _{0.2} Al ₁	[56]	Master
Fabrication of Nanowires via High-Entropy Powders	2004	Al-Cr-Fe-Ni-Si-Ti-Zr	[49]	Master
Research for the Adhesive Wear Properties of Al _x CoCuFeNiTi _y High-Entropy Alloys	2004	Al _x Co-Cu-Fe-Ni-Ti _y	[58]	Master
Particle Erosion Characteristics of a Plasma-Sprayed Zr-Based High-Entropy Alloy	2004	Zr-Based High-Entropy Alloy	[52]	Master

3. Mechanical Properties of High-Entropy Alloys

High-entropy alloys have been found to have great mechanical properties [3], especially at cryogenic [5] and elevated temperatures [6]. It has been reported that the temperature-dependent mechanical properties can be influenced by both entropy and element effects [42]. The identification of the high-entropy effects is an emerging research area.

For soft materials, the temperature-associated entropy effects for thermoelastic behavior can be found as follows:

$$f = f_U + f_S = \left(\frac{\partial U}{\partial l} \right)_{V,T} - T \left(\frac{\partial S}{\partial l} \right)_{V,T} = \left(\frac{\partial U}{\partial l} \right)_{V,T} + T \left(\frac{\partial f}{\partial l} \right)_{V,T} \quad (1)$$

where f is the total elastic force, f_U is the component of the internal energy, f_S is the component of the entropic energy, U is the internal energy, S is the entropy of the system, and T is the temperature. The force at a fixed strain increases with temperature, with the force being nearly proportional to the absolute temperature.

For the deoxyribonucleic acids [63], there could be conformational entropy effects, as presented in Equation (2):

$$\frac{FA}{kT} = \frac{1}{4\left(1 - \frac{x}{L}\right)^2} - \frac{1}{4} + \frac{x}{L} \quad (2)$$

where F is the force as a function of the extension, x , A is the length of the deoxyribonucleic acid, k is the Boltzmann's constant, T is the temperature, and L is the molecular contour length. The elastic behavior of Actin networks is an example of such a concurrent effect from the entropy-driven and energy-driven elasticities [64,65]. It is interesting to re-think if these entropy effects act on the high-entropy alloys as well.

For general metallic systems, the deformation mechanisms are functions of their strength and ductility; they are categorized in some classic models, as listed below. For example, a homogeneous plastic response with the irreversible flow of strain hardening indicates the dislocation movement, which can be shown as the Hollomon relationship:

$$\sigma_{true} = K\epsilon_{true}^n \quad (3)$$

where σ_{true} is the true stress, K is a material constant, and n is the strain-hardening coefficient. For a heterogeneous plastic response, the phenomenon could be from twinning and/or a vacancy interaction with dislocations. For a heterogeneous plastic and homogeneous plastic response, there could be dislocation–solute atom interactions showing upper and lower yield strengths as a Lüder band.

Specifically, yield strength (σ_y) is a combination of the frictional stress (σ_{fr}), the effects of solid solutions (σ_{ss}), dislocation density (σ_ρ), precipitate hardening ($\sigma_{precipitate}$), and grain boundaries (σ_{gb}), as summarized in the following equation:

$$\sigma_y = \sigma_{fr} + \sigma_{ss} + \sigma_\rho + \sigma_{precipitate} + \sigma_{gb}. \quad (4)$$

As mentioned above, the yield and tensile strength, ductility, fracture toughness, and creep and fatigue strengths are microstructure-sensitive mechanical properties [8].

For high-entropy alloys, a major characteristic is its low stacking fault energies (SFE) [21]. Huang et al. examined the SFE as a function of temperature via ab initio calculations [20]. Their models consider chemical, magnetic, and strain contributions. The local structural energies, magnetic moments, and elastic moduli predicted deformation twins and face-centered-cubic to hexagonal-phase transformation under cryogenic conditions [20]. The twinning results agree with earlier experimental results [5]. Their predictions for phase transformation have been experimentally validated [15,66–68].

Niu et al.'s experimental and simulation results depict the possible paths for the aforementioned microstructure-dependent phase-transformation mechanisms [22]. They reveal the interactions between magnetic and mechanical properties of CrCoNi and other equiatomic ternary derivatives of CrMnFeCoNi. Niu et al. demonstrated that magnetically frustrated Mn eliminates the Face-Centered Cubic (FCC)–Hexagonal Closest Packed (HCP) energy difference as an important element effect for high-entropy alloys [22].

In summary, the element effect can contribute to local heterogeneous atomic sizes, electronegativity [9], and magnetic properties [20,22] of the high-entropy alloys among the elements. These differences result in low stacking fault energies [20,21], twinning [5,42], and phase transformation [3,15,30,43,66–70], which accommodate the deformation and enhance the overall performance in terms of strength and ductility.

4. Combinatorial Approaches for Magnetic Features

Nowadays, most of the electronics and computational devices facilitate magnetism and magnetic materials as the smart functional materials [71]. The excellent mechanical properties of high-entropy alloys can improve the reliability of these modern devices [72–74].

The magnetic materials are classified as either soft or hard from their magnetization hysteresis characteristics.

Ferromagnetic and ferrimagnetic materials contain specific elements that have large magnetic moments. The high-entropy alloys containing these elements and their combinatorial properties focusing on magnetic and mechanical properties are summarized in Table 2.

Here, the magnetic properties of particular concern are the remanent induction (T) and coercive field (A/m). Figure 4 presents a comparison between several commercial magnets and selected high-entropy alloys. The commercial soft and hard magnets are shown in the regions marked with solid lines. The high-entropy alloys are presented in the regions marked with symbols.

The two most important characteristics for applications of soft and hard magnetic materials are the coercivity and what is termed as the energy product, designated as BH_{max} . Soft magnets have low coercive fields and narrow hysteresis loops. Hard magnets have much higher coercive fields. Larger maximum energy products (BH_{max} , unit $\frac{J}{m^3}$) are desirable for hard magnets. The maximum energy product depends on the shape of the B–H curve. However, for a given shape, it increases with the product of $B_R \times H_C$ (the diagonals on Figure 4). The remanent induction, B_R , is the induction that remains when the field, H , is removed. The coercive field, H_C , is the field required to fully magnetize and demagnetize the material.

Table 2. Summary of high-entropy alloys (HEAs) and complex concentrated alloys (CCAs) for magnetic applications.

HEA System	Properties	Year	Title	Reference
AlCoCrFeNiNbx	Yield Strength	2012	Effect of Nb addition on the microstructure and properties of AlCoCrFeNi high-entropy alloy.	[32]
	Young's Modulus	2012	Effect of Nb addition on the microstructure and properties of AlCoCrFeNi high-entropy alloy.	[32]
AlxCoFeNi	Coercive Force H_c	2014	Effects of Al and Si addition on the structure and properties of CoFeNi equal atomic ratio alloy	[43]
	Remanent Induction B_r	2014	Effects of Al and Si addition on the structure and properties of CoFeNi equal atomic ratio alloy	[43]
	Yield Strength	2014	Effects of Al and Si addition on the structure and properties of CoFeNi equal atomic ratio alloy	[43]
	Young's Modulus	2014	Effects of Al and Si addition on the structure and properties of CoFeNi equal atomic ratio alloy	[43]
AlxCoCrFeNi	Coercive Force H_c	2017	A combinatorial approach for assessing the magnetic properties of high entropy alloys: Role of Cr in AlCo _x Cr _{1-x} FeNi	[75]
	Remanent Induction B_r	2017	A combinatorial approach for assessing the magnetic properties of high entropy alloys: Role of Cr in AlCo _x Cr _{1-x} FeNi	[75]
	Yield Strength	2017	Dual-phase high-entropy alloys for high-temperature structural applications	[33]
	Young's Modulus	2015	Plastic deformation of Al _{0.3} CoCrFeNi and AlCoCrFeNi high-entropy alloys under nanoindentation	[34]
		2009	Microstructure and mechanical property of as-cast, -homogenized, and -deformed AlxCoCrFeNi (0 ≤ x ≤ 2) high-entropy alloys	[35]
AlCoCrCuFeNi	Yield Strength	2012	Tensile properties of an AlCrCuNiFeCo high-entropy alloy in as-cast and wrought conditions	[36]
		2013	Phase composition and superplastic behavior of a wrought AlCoCrCuFeNi high-entropy alloy	[37]
	Young's Modulus	2012	Effect of elemental interaction on microstructure and mechanical properties of FeCoNiCuAl alloys	[38]
		2008	Effects of Mn, Ti and V on the microstructure and properties of AlCrFeCoNiCu high entropy alloy	[39]

Table 2. Cont.

HEA System	Properties	Year	Title	Reference
CoCrFeNiMn	Coercive Force H_c	2017	Tailoring magnetic behavior of CoFeMnNiX (X = Al, Cr, Ga, and Sn) high entropy alloys by metal doping	[76]
	Remanent Induction B_r	2017	Tailoring magnetic behavior of CoFeMnNiX (X = Al, Cr, Ga, and Sn) high entropy alloys by metal doping	[76]
	Yield Strength	2014	A fracture-resistant high-entropy alloy for cryogenic applications	[5]
		2013	The influences of temperature and microstructure on the tensile properties of a CoCrFeMnNi high-entropy alloy	[44]
	Young's Modulus	2018	Variations of the elastic properties of the CoCrFeMnNi high entropy alloy deformed by groove cold rolling	[40]
CoCrFeNi	Yield Strength	2013	Tensile properties of high- and medium-entropy alloys	[41]
	Young's Modulus	2014	Temperature dependence of the mechanical properties of equiatomic solid solution alloys with face-centered cubic crystal structures	[42]
CoCrMnNi	Yield Strength	2014	Temperature dependence of the mechanical properties of equiatomic solid solution alloys with face-centered cubic crystal structures	[42]
	Young's Modulus	2014	Temperature dependence of the mechanical properties of equiatomic solid solution alloys with face-centered cubic crystal structures	[42]
CoFeMnNi	Yield Strength	2014	Temperature dependence of the mechanical properties of equiatomic solid solution alloys with face-centered cubic crystal structures	[42]
	Young's Modulus	2014	Temperature dependence of the mechanical properties of equiatomic solid solution alloys with face-centered cubic crystal structures	[42]
CoFeNiSix	Coercive Force H_c	2014	Effects of Al and Si addition on the structure and properties of CoFeNi equal atomic ratio alloy	[43]
	Remanent Induction B_r	2014	Effects of Al and Si addition on the structure and properties of CoFeNi equal atomic ratio alloy	[43]
	Yield Strength	2014	Effects of Al and Si addition on the structure and properties of CoFeNi equal atomic ratio alloy	[43]
	Young's Modulus	2014	Effects of Al and Si addition on the structure and properties of CoFeNi equal atomic ratio alloy	[43]

Table 2. Cont.

HEA System	Properties	Year	Title	Reference
CoFeNi(MnAl) _x	Coercive Force H_c	2017	Composition dependence of structure, physical and mechanical properties of FeCoNi(MnAl) _x high entropy alloys	[77]
	Remanent Induction B_r	2017	Composition dependence of structure, physical and mechanical properties of FeCoNi(MnAl) _x high entropy alloys	[77]
	Yield Strength	2017	Composition dependence of structure, physical and mechanical properties of FeCoNi(MnAl) _x high entropy alloys	[77]
CoFeNi(AlSi) _x	Coercive Force H_c	2013	High-entropy alloys with high saturation magnetization, electrical resistivity, and malleability	[27]
	Remanent Induction B_r	2013	High-entropy alloys with high saturation magnetization, electrical resistivity, and malleability	[27]
	Yield Strength	2019	Compositional design of soft magnetic high entropy alloys by minimizing magnetostriction coefficient in (Fe _{0.3} Co _{0.5} Ni _{0.2}) _{100-x} (Al _{1/3} Si _{2/3}) _x system	[72]
	Young's Modulus	2017	Effects of short-range order on the magnetic and mechanical properties of FeCoNi(AlSi) _x high entropy alloys	[78]
Al _x CrCuFeNi ₂	Coercive Force H_c	2016	A combinatorial assessment of Al _x CrCuFeNi ₂ (0 < x < 1.5) complex concentrated alloys: Microstructure, microhardness, and magnetic properties	[29]
	Remanent Induction B_r	2016	A combinatorial assessment of Al _x CrCuFeNi ₂ (0 < x < 1.5) complex concentrated alloys: Microstructure, microhardness, and magnetic properties	[29]
	Yield Strength	2016	Strain rate effects on the dynamic mechanical properties of the AlCrCuFeNi ₂ high-entropy alloy	[79]
	Young's Modulus	2012	Microstructure and properties of AlCrFeCuNi _x (0.6 ≤ x ≤ 1.4) high-entropy alloys	[80]
AlCo _x Cr _{1-x} FeNi	Coercive Force H_c	2017	A combinatorial approach for assessing the magnetic properties of high entropy alloys: Role of Cr in AlCo _x Cr _{1-x} FeNi	[75]
	Remanent Induction B_r	2017	A combinatorial approach for assessing the magnetic properties of high entropy	[75]

Table 2. Cont.

HEA System	Properties	Year	Title	Reference
CoFeMnNiGa	Coercive Force H_c	2017	Tailoring magnetic behavior of CoFeMnNiX (X = Al, Cr, Ga, and Sn) high entropy alloys by metal doping	[76]
	Remanent Induction B_r	2017	Tailoring magnetic behavior of CoFeMnNiX (X = Al, Cr, Ga, and Sn) high entropy alloys by metal doping	[76]
CoFeMnNiAl	Coercive Force H_c	2017	Tailoring magnetic behavior of CoFeMnNiX (X = Al, Cr, Ga, and Sn) high entropy alloys by metal doping	[76]
	Remanent Induction B_r	2017	Tailoring magnetic behavior of CoFeMnNiX (X = Al, Cr, Ga, and Sn) high entropy alloys by metal doping	[76]
Other HEAs	Coercive Force H_c	2012	Microstructure and magnetic properties of FeNiCuMnTiSnx high entropy alloys	[81]
	Remanent Induction B_r	2012	Microstructure and magnetic properties of FeNiCuMnTiSnx high entropy alloys	[81]
CCA System	Properties	Year	Title	Reference
Commercial Soft Magnets	Coercive Force H_c	2003	Metals Handbook, Desk Edition 2nd Edition I	[82]
	Remanent Induction B_r	2003	Metals Handbook, Desk Edition 2nd Edition I	[82]
Commercial Hard Magnets	Coercive Force H_c	2003	Metals Handbook, Desk Edition 2nd Edition I	[82]
	Remanent Induction B_r	2003	Metals Handbook, Desk Edition 2nd Edition I	[82]

5. Mechanical and Magnetic Maps for the Applications of High-Entropy Alloys

Magnetic materials are important in several areas, such as information storage, superconductivity, electrical-power transmission, high-speed switching, high-speed-signal transmission for computation, and high-speed magnetically-levitated trains. Many of these applications require excellent mechanical properties across various operating temperatures, areas where high-entropy alloys show great potential. For example, there are both active and passive electromagnetic devices for vibration damping and isolation, and the selection criteria for materials and for these devices include the coercivity, remanence, relative permeability, and saturation field [83].

Here, we compare different combinations of mechanical and magnetic properties, and we select several potential applications and their featured combinations of properties. Magnets embedded in the discs for regenerative braking induces a current and allows power to be drawn to the electric motor that drives the wheels. There are several material requirements for this application, such as the density, thermal conductivity, thermal expansion, hardness, Poisson's ratio, and Young's modulus [84], while the maximum energy product (BH_{max} , units $\frac{J}{m^3}$) is also important. For these applications, Young's modulus–coercive force and Young's modulus–remanent induction relationships are summarized in Figure 5; Figure 6, respectively.

For magnetic applications requiring high strength, such as magnetic windings, a higher strength is needed before mechanical failure. Furthermore, low heat generation during operation while maximizing the magnetic field is required. For these multiple constraints [85], high-entropy alloys

also show great potential [86]. Figures 2 and 3 exhibit the yield strength–coercive force and yield strength–remnant induction relationships, respectively.

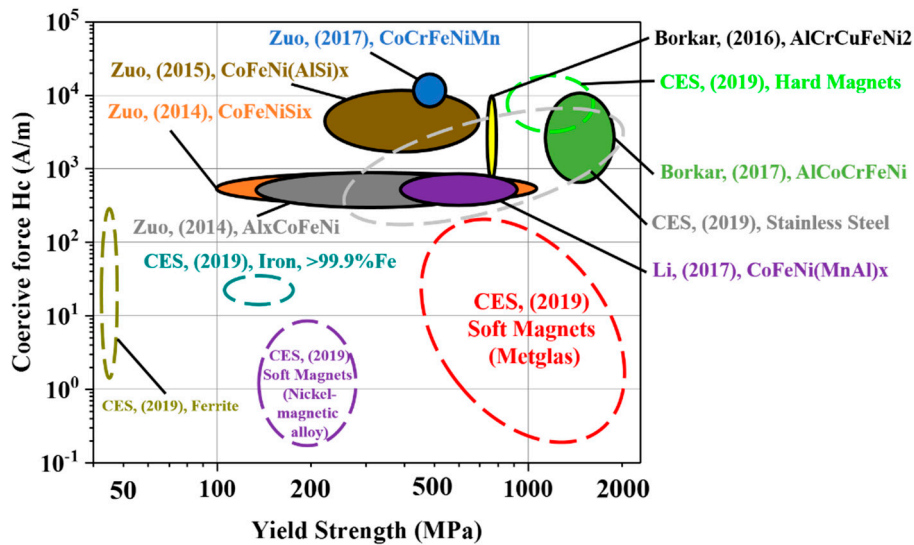


Figure 2. Coercive force vs. yield strength for conventional alloys (encircled by dashed lines) and HEAs (colored regions encircled by solid lines). (Data taken from [5,27,29,33,43,44,72,76,77,79,80]). The data is from the CES EduPack 2009, Granta Design, Limited, Cambridge, UK, 2009.

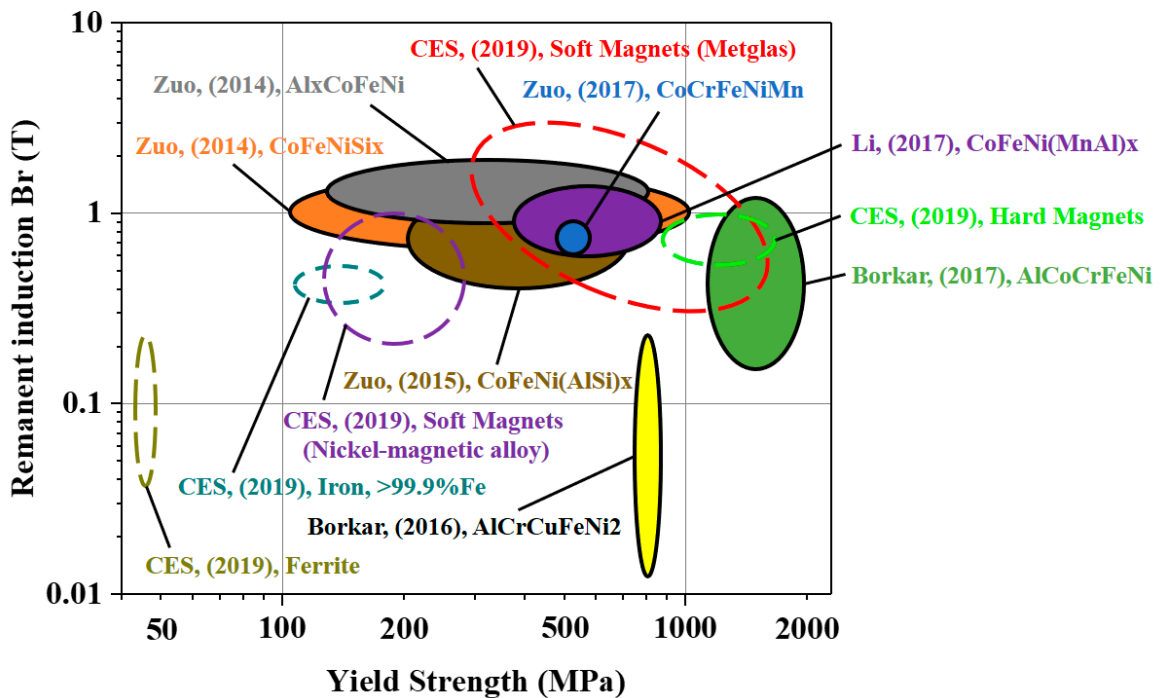


Figure 3. Remanent induction vs. yield strength for conventional alloys (encircled by dashed lines) and HEAs (colored regions encircled by solid lines). (Data taken from [5,27,29,33,43,44,72,76,77,79,80]). The data is from the CES EduPack 2009, Granta Design, Limited, Cambridge, UK, 2009.

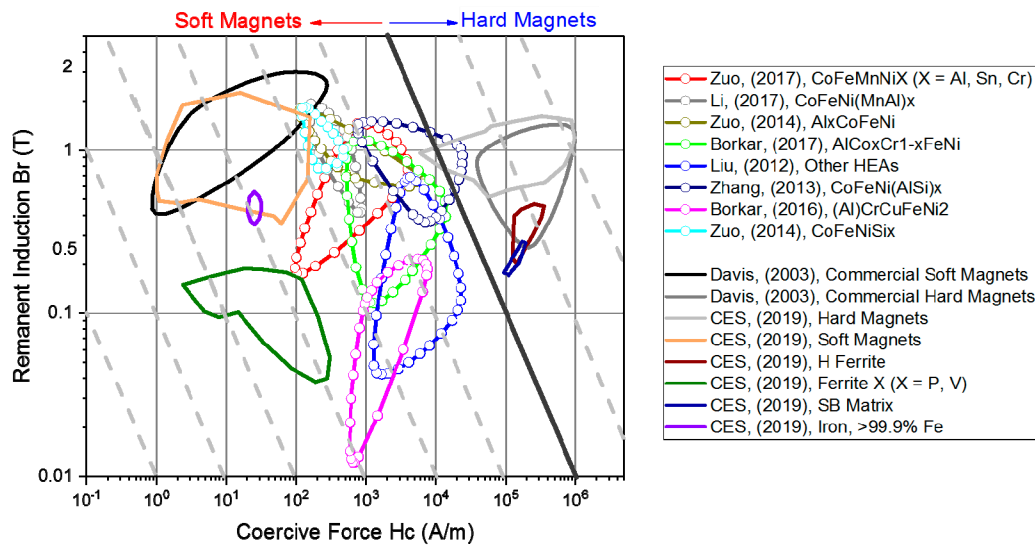


Figure 4. Material property spaces for HEAs and CCAs, comparing remanent induction vs. coercive force for conventional metal alloys (lines) and HEAs (symbols). (Data taken from [27,29,43,75–77,81,82]). The data is from the CES EduPack 2009, Granta Design, Limited, Cambridge, UK, 2009.

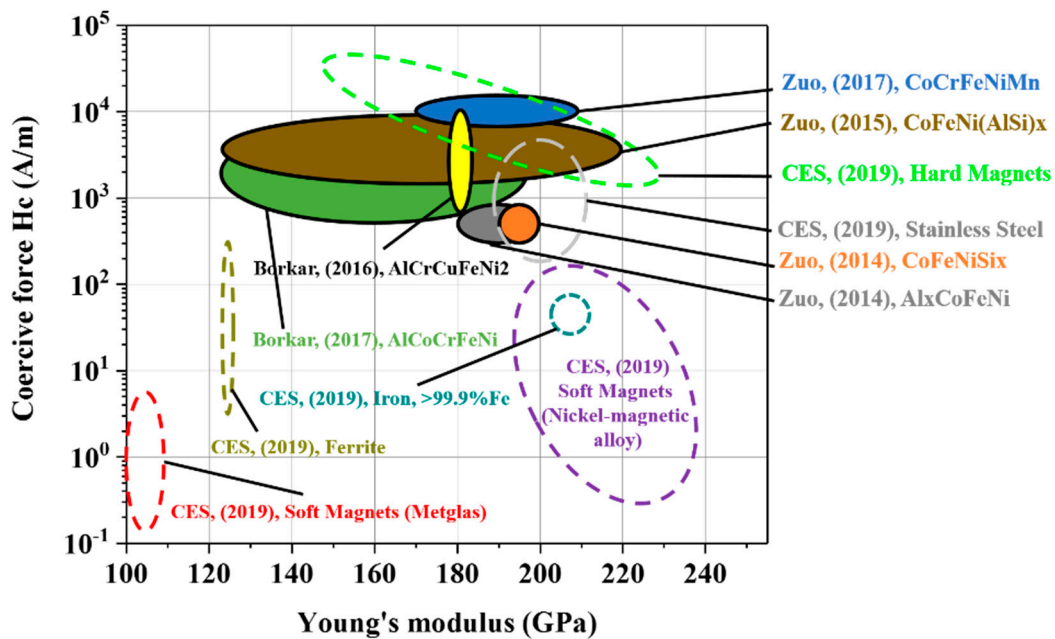


Figure 5. Coercive force vs. Young's modulus for conventional alloys (encircled by dashed lines) and HEAs (colored regions encircled by solid lines). (Data taken from [27,29,34,35,40,43,75,76,78,80]). The data is from the CES EduPack 2009, Granta Design, Limited, Cambridge, UK, 2009.

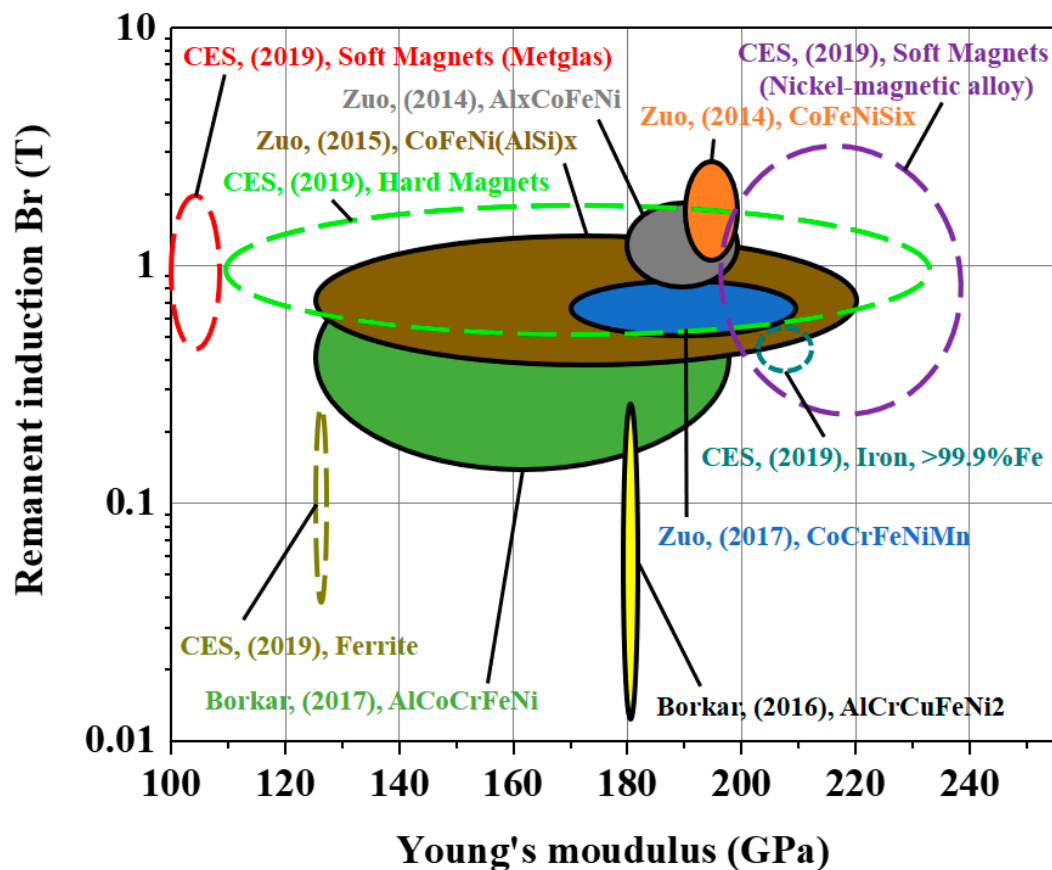


Figure 6. Remanent induction vs. Young's modulus for conventional alloys (encircled by dashed lines) and HEAs (colored regions encircled by solid lines). (Data taken from [27,29,34,35,40,43,75,76,78,80]). The data is from the CES EduPack 2009, Granta Design, Limited, Cambridge, UK, 2009.

6. Discussion and Future Perspectives

As shown by the blue arrow in Figure 4, all of the hard magnets made from commercial alloys have products of the remanent induction (B_R) and coercive field (H_C) greater than those of the high-entropy alloys. Similarly, as shown by the red arrow, commercial alloys have better soft-magnet performance, with small products of $B_R \times H_C$, as presented by the diagonals in Figure 4.

However, when applications require a specific function needing more than the optimization of a single property, high-entropy alloys present combinatorial advantages since the alloys are much more diverse, as demonstrated in Figure 5, Figure 6, Figure 2, Figure 3, as compared with the narrow regions shown in Figure 4.

Specific functional applications need different combinatorial advantages. For example, to improve the thermoelastic-type shape memory, metallic systems require slow diffusion and resistance to plastic deformation. Moreover, it is important for shape-memory alloys to accumulate more reversible martensitic deformation. Firstov et al. [87] reported TiZrHfCoNiCu high-entropy alloys for the shape-memory effect. The mechanisms of the reversible-deformation-induced martensitic transformation of the Al_{0.6}CoCrFeNi high-entropy alloy were revealed by in situ synchrotron X-ray measurements [88].

Another example is the development of high-entropy alloys for thermoelectric applications. Specifically, to satisfy the thermoelectric functions, one criterion for selecting the material is the low thermal conductivity for improving the Seebeck coefficient. Fan et al. showed that the severe lattice distortion of high-entropy alloys has strong potential in this regard [89].

Finally, the developments of the additive manufacturing enable the metals for better performance [90]. The additive manufacturing brings high degrees of geometrical freedom to the production of alloy components [91]. The advantages of the additive manufacturing, such as customized geometry [92], fast cooling for intermediate phase effects [93], mixing of metallics-ceramics powders [94,95], and anisotropic effects [96], are well known. For additive manufacturing, high-entropy alloys also show great potentials [97–100].

7. Conclusions

This article explores the state of high-entropy alloys and their combinatorial approaches mainly for magnetic applications. Several earlier high-entropy-alloy studies in the areas of thin film, magnetic behavior, nanowires, thermal-spray coating, plasma spraying, corrosion behavior, welding, inclusion effects, and wear properties are summarized. High-entropy alloy systems that were reported for both their mechanical and magnetic properties were compared via the combination of their Young's modulus, yield strength, remanent induction, and coercive force. Several potential applications requiring both mechanical and magnetic properties were reported. The objective of this article was to review the reported mechanical and magnetic properties of high-entropy alloys for more combinatorial advances. Several advanced measurements using neutron and synchrotron were also included, along with examples of machine learning used for the design of high-entropy alloys.

Author Contributions: Conceptualization, E.-W.H.; validation, P.K.L.; resources, E.-W.H.; data curation, G.-Y.H., S.Y.L., J.J. and K.-P.C., J.J.C.; writing—review and editing, W.-C.Y.; supervision, E.-W.H.; funding acquisition, E.-W.H. All authors have read and agreed to the published version of the manuscript.

Funding: The present work was supported by the Ministry of Science and Technology (MOST) Programs [grant numbers 107-2628-E-009-001-MY3, 107-2218-E-009-003, 108-3017-F-009-003, and 108-2221-E-009-131-MY4]; and "Center for Semiconductor Technology Research" from the Featured Areas Research Center Program within the framework of the Higher Education Sprout Project by the Ministry of Education (MOE) in Taiwan.

Acknowledgments: E.W.H. is grateful for the financial support of the Ministry of Science and Technology Program nos. 107-2628-E-009-001-MY3, 107-2218-E-009-003, 107-3017-F-007-003, and 108-2221-E-009-131-MY4. The work was financially supported by the "High Entropy Materials Center" from The Featured Areas Research Center Program within the framework of the Higher Education Sprout Project of the Ministry of Education in Taiwan. P.K.L. appreciates support from the US Army Research Office Project nos. W911NF-13-1-0438 and W911NF-19-2-0049 with program managers M.P. Bakas, S.N. Mathaudhu, and D.M. Stepp. P.K.L. thanks the National Science Foundation DMR-1611180 and 1809640 with program directors, J. Yang, G. Shiflet and D. Farkas. SYL was supported by National Research Foundation (NRF) grant funded by the Korean Government, 2019R1H1A2080092 and 2020M2A2A6A05026873.

Conflicts of Interest: The authors declare no conflict of interest.

References

1. Yeh, J.-W.; Chen, S.-K.; Lin, S.-J.; Gan, J.-Y.; Chin, T.-S.; Shun, T.-T.; Tsau, C.-H.; Chang, S.-Y. Nanostructured high-entropy alloys with multiple principal elements: Novel alloy design concepts and outcomes. *Adv. Eng. Mater.* **2004**, *6*, 299–303. [[CrossRef](#)]
2. Cantor, B.; Chang, I.T.H.; Knight, P.; Vincent, A.J.B. Microstructural development in equiatomic multicomponent alloys. *Mater. Sci. Eng. A* **2004**, *375–377*, 213–218. [[CrossRef](#)]
3. Miracle, D.B.; Senkov, O.N. A critical review of high entropy alloys and related concepts. *Acta Mater.* **2017**, *122*, 448–511. [[CrossRef](#)]
4. Diao, H.Y.; Feng, R.; Dahmen, K.A.; Liaw, P.K. Fundamental deformation behavior in high-entropy alloys: An overview. *Curr. Opin. Solid State Mater. Sci.* **2017**, *21*, 252–266. [[CrossRef](#)]
5. Gludovatz, B.; Hohenwarter, A.; Catoor, D.; Chang, E.H.; George, E.P.; Ritchie, R.O. A fracture-resistant high-entropy alloy for cryogenic applications. *Science* **2014**, *345*, 1153–1158. [[CrossRef](#)]
6. Senkov, O.N.; Wilks, G.B.; Miracle, D.B.; Chuang, C.P.; Liaw, P.K. Refractory high-entropy alloys. *Intermetallics* **2010**, *18*, 1758–1765. [[CrossRef](#)]
7. Huang, E.W.; Liaw, P.K. High-temperature materials for structural applications: New perspectives on high-entropy alloys, bulk metallic glasses, and nanomaterials. *MRS Bull.* **2019**, *44*, 847–853. [[CrossRef](#)]

8. Jones, D.R.H.; Ashby, M.F. *Engineering Materials 2: An Introduction to Microstructures, Processing and Design*; Elsevier Science: Amsterdam, The Netherlands, 2005.
9. Ding, Q.; Zhang, Y.; Chen, X.; Fu, X.; Chen, D.; Chen, S.; Gu, L.; Wei, F.; Bei, H.; Gao, Y.; et al. Tuning element distribution, structure and properties by composition in high-entropy alloys. *Nature* **2019**, *574*, 223–227. [[CrossRef](#)]
10. Zhang, Y.; Zuo, T.T.; Tang, Z.; Gao, M.C.; Dahmen, K.A.; Liaw, P.K.; Lu, Z.P. Microstructures and properties of high-entropy alloys. *Prog. Mater. Sci.* **2014**, *61*, 1–93. [[CrossRef](#)]
11. Ma, S.G.; Zhang, S.F.; Gao, M.C.; Liaw, P.K.; Zhang, Y. A successful synthesis of the CoCrFeNiAl_{0.3} single-crystal, high-entropy alloy by bridgman solidification. *JOM* **2013**, *65*, 1751–1758. [[CrossRef](#)]
12. Brif, Y.; Thomas, M.; Todd, I. The use of high-entropy alloys in additive manufacturing. *Scr. Mater.* **2015**, *99*, 93–96. [[CrossRef](#)]
13. Santodonato, L.J.; Zhang, Y.; Feyngenson, M.; Parish, C.M.; Gao, M.C.; Weber, R.J.K.; Neuefeind, J.C.; Tang, Z.; Liaw, P.K. Deviation from high-entropy configurations in the atomic distributions of a multi-principal-element alloy. *Nat. Commun.* **2015**, *6*, 5964. [[CrossRef](#)] [[PubMed](#)]
14. Woo, W.; Huang, E.W.; Yeh, J.-W.; Choo, H.; Lee, C.; Tu, S.-Y. In-situ neutron diffraction studies on high-temperature deformation behavior in a CoCrFeMnNi high entropy alloy. *Intermetallics* **2015**, *62*, 1–6. [[CrossRef](#)]
15. Huang, E.W.; Lin, C.-M.; Juang, J.-Y.; Chang, Y.-J.; Chang, Y.-W.; Wu, C.-S.; Tsai, C.-W.; Yeh, A.-C.; Shieh, S.R.; Wang, C.-P.; et al. Deviatoric deformation kinetics in high entropy alloy under hydrostatic compression. *J. Alloys Compd.* **2019**, *792*, 116–121. [[CrossRef](#)]
16. Lam, T.-N.; Chou, Y.-S.; Chang, Y.-J.; Sui, T.-R.; Yeh, A.-C.; Harjo, S.; Lee, S.Y.; Jain, J.; Lai, B.-H.; Huang, E.-W. Comparing cyclic tension-compression effects on CoCrFeMnNi high-entropy alloy and ni-based superalloy. *Crystals* **2019**, *9*, 420. [[CrossRef](#)]
17. Zhao, J.-C.; Zheng, X.; Cahill, D.G. High-throughput measurements of materials properties. *JOM* **2011**, *63*, 40–44. [[CrossRef](#)]
18. Zhao, J.-C. High-throughput experimental tools for the materials genome initiative. *Chin. Sci. Bull.* **2014**, *59*, 1652–1661. [[CrossRef](#)]
19. Widom, M.; Huhn, W.P.; Maiti, S.; Steurer, W. Hybrid monte carlo/molecular dynamics simulation of a refractory metal high entropy alloy. *Metall. Mater. Trans. A* **2014**, *45*, 196–200. [[CrossRef](#)]
20. Huang, S.; Li, W.; Lu, S.; Tian, F.; Shen, J.; Holmström, E.; Vitos, L. Temperature dependent stacking fault energy of FeCrCoNiMn high entropy alloy. *Scr. Mater.* **2015**, *108*, 44–47. [[CrossRef](#)]
21. Zhang, Y.H.; Zhuang, Y.; Hu, A.; Kai, J.J.; Liu, C.T. The origin of negative stacking fault energies and nano-twin formation in face-centered cubic high entropy alloys. *Scr. Mater.* **2017**, *130*, 96–99. [[CrossRef](#)]
22. Niu, C.; LaRosa, C.R.; Miao, J.; Mills, M.J.; Ghazisaeidi, M. Magnetically-driven phase transformation strengthening in high entropy alloys. *Nat. Commun.* **2018**, *9*, 1363. [[CrossRef](#)] [[PubMed](#)]
23. Kim, G.; Diao, H.; Lee, C.; Samaei, A.T.; Phan, T.; de Jong, M.; An, K.; Ma, D.; Liaw, P.K.; Chen, W. First-principles and machine learning predictions of elasticity in severely lattice-distorted high-entropy alloys with experimental validation. *Acta Mater.* **2019**, *181*, 124–138. [[CrossRef](#)]
24. Chang, Y.-J.; Jui, C.-Y.; Lee, W.-J.; Yeh, A.-C. Prediction of the composition and hardness of high-entropy alloys by machine learning. *JOM* **2019**, *71*, 3433–3442. [[CrossRef](#)]
25. Koželj, P.; Vrtnik, S.; Jelen, A.; Jazbec, S.; Jagličić, Z.; Maiti, S.; Feuerbacher, M.; Steurer, W.; Dolinšek, J. Discovery of a superconducting high-entropy alloy. *Phys. Rev. Lett.* **2014**, *113*, 107001. [[CrossRef](#)] [[PubMed](#)]
26. Xie, P.; Yao, Y.; Huang, Z.; Liu, Z.; Zhang, J.; Li, T.; Wang, G.; Shahbazian-Yassar, R.; Hu, L.; Wang, C. Highly efficient decomposition of ammonia using high-entropy alloy catalysts. *Nat. Commun.* **2019**, *10*, 4011. [[CrossRef](#)] [[PubMed](#)]
27. Zhang, Y.; Zuo, T.; Cheng, Y.; Liaw, P.K. High-entropy alloys with high saturation magnetization, electrical resistivity, and malleability. *Sci. Rep.* **2013**, *3*, 1455. [[CrossRef](#)] [[PubMed](#)]
28. Zuo, T.; Zhang, M.; Liaw, P.K.; Zhang, Y. Novel high entropy alloys of Fe_xCo_{1-x}NiMnGa with excellent soft magnetic properties. *Intermetallics* **2018**, *100*, 1–8. [[CrossRef](#)]
29. Borkar, T.; Gwalani, B.; Choudhuri, D.; Mikler, C.V.; Yannetta, C.J.; Chen, X.; Ramanujan, R.V.; Styles, M.J.; Gibson, M.A.; Banerjee, R. A combinatorial assessment of Al_xCrCuFeNi₂ (0 < x < 1.5) complex concentrated alloys: Microstructure, microhardness, and magnetic properties. *Acta Mater.* **2016**, *116*, 63–76. [[CrossRef](#)]

30. Li, Z.; Pradeep, K.G.; Deng, Y.; Raabe, D.; Tasan, C.C. Metastable high-entropy dual-phase alloys overcome the strength–ductility trade-off. *Nature* **2016**, *534*, 227. [[CrossRef](#)]
31. Yang, T.; Zhao, Y.L.; Tong, Y.; Jiao, Z.B.; Wei, J.; Cai, J.X.; Han, X.D.; Chen, D.; Hu, A.; Kai, J.J.; et al. Multicomponent intermetallic nanoparticles and superb mechanical behaviors of complex alloys. *Science* **2018**, *362*, 933–937. [[CrossRef](#)]
32. Ma, S.G.; Zhang, Y. Effect of Nb addition on the microstructure and properties of AlCoCrFeNi high-entropy alloy. *Mater. Sci. Eng. A* **2012**, *532*, 480–486. [[CrossRef](#)]
33. Lim, K.R.; Lee, K.S.; Lee, J.S.; Kim, J.Y.; Chang, H.J.; Na, Y.S. Dual-phase high-entropy alloys for high-temperature structural applications. *J. Alloys Compd.* **2017**, *728*, 1235–1238. [[CrossRef](#)]
34. Jiao, Z.-M.; Ma, S.-G.; Yuan, G.-Z.; Wang, Z.-H.; Yang, H.-J.; Qiao, J.-W. Plastic deformation of Al_{0.3}CoCrFeNi and AlCoCrFeNi high-entropy alloys under nanoindentation. *J. Mater. Eng. Perform.* **2015**, *24*, 3077–3083. [[CrossRef](#)]
35. Kao, Y.-F.; Chen, T.-J.; Chen, S.-K.; Yeh, J.-W. Microstructure and mechanical property of as-cast, -homogenized, and -deformed Al_xCoCrFeNi (0 ≤ x ≤ 2) high-entropy alloys. *J. Alloys Compd.* **2009**, *488*, 57–64. [[CrossRef](#)]
36. Kuznetsov, A.V.; Shaysultanov, D.G.; Stepanov, N.D.; Salishchev, G.A.; Senkov, O.N. Tensile properties of an AlCrCuNiFeCo high-entropy alloy in as-cast and wrought conditions. *Mater. Sci. Eng. A* **2012**, *533*, 107–118. [[CrossRef](#)]
37. Shaysultanov, D.G.; Stepanov, N.D.; Kuznetsov, A.V.; Salishchev, G.A.; Senkov, O.N. Phase composition and superplastic behavior of a wrought AlCoCrCuFeNi high-entropy Alloy. *JOM* **2013**, *65*, 1815–1828. [[CrossRef](#)]
38. Zhuang, Y.X.; Liu, W.J.; Chen, Z.Y.; Xue, H.D.; He, J.C. Effect of elemental interaction on microstructure and mechanical properties of FeCoNiCuAl alloys. *Mater. Sci. Eng. A* **2012**, *556*, 395–399. [[CrossRef](#)]
39. Li, B.S.; Wang, Y.P.; Ren, M.X.; Yang, C.; Fu, H.Z. Effects of Mn, Ti and V on the microstructure and properties of AlCrFeCoNiCu high entropy alloy. *Mater. Sci. Eng. A* **2008**, *498*, 482–486. [[CrossRef](#)]
40. Lohmuller, P.; Peltier, L.; Hazotte, A.; Zollinger, J.; Laheurte, P.; Fleury, E. Variations of the elastic properties of the CoCrFeMnNi High entropy alloy deformed by groove cold rolling. *Materials* **2018**, *11*, 1337. [[CrossRef](#)]
41. Gali, A.; George, E.P. Tensile properties of high- and medium-entropy alloys. *Intermetallics* **2013**, *39*, 74–78. [[CrossRef](#)]
42. Wu, Z.; Bei, H.; Pharr, G.M.; George, E.P. Temperature dependence of the mechanical properties of equiatomic solid solution alloys with face-centered cubic crystal structures. *Acta Mater.* **2014**, *81*, 428–441. [[CrossRef](#)]
43. Zuo, T.T.; Li, R.B.; Ren, X.J.; Zhang, Y. Effects of Al and Si addition on the structure and properties of CoFeNi equal atomic ratio alloy. *J. Magn. Magn. Mater.* **2014**, *371*, 60–68. [[CrossRef](#)]
44. Otto, F.; Dlouhý, A.; Somsen, C.; Bei, H.; Eggeler, G.; George, E.P. The influences of temperature and microstructure on the tensile properties of a CoCrFeMnNi high-entropy alloy. *Acta Mater.* **2013**, *61*, 5743–5755. [[CrossRef](#)]
45. Chen, Y.U. NiAlFeCuCoCr-6-Component Alloy Metal Films Structure. Master's Thesis, Chinese Culture University, Taipei City, Taiwan, 2002.
46. Tsai, M.-H. Study on the Microstructure and Electrical Properties Evolution of High-Entropy Alloy Thin Films. Master's Thesis, National Tsing Hua University, Hsinchu City, Taiwan, 2003.
47. Lin, P.-C. Development on the High Frequency Soft-Magnetic Thin Films from High-Entropy Alloys. Master's Thesis, National Tsing Hua University, Hsinchu City, Taiwan, 2003.
48. Yu, C.-H. Research on the Bulks and Thin Film Properties of CrMoNbTiZr High-Entropy Alloys. Master's Thesis, Chinese Culture University, Taipei City, Taiwan, 2004.
49. Wu, N.F. Fabrication of Nanowires via High-Entropy Powders. Master's Thesis, National Tsing Hua University, Hsinchu City, Taiwan, 2004.
50. Jiayu, C. Development of Multicomponent High-Entropy Alloys for Thermal Spray Coating. Master's Thesis, National Tsing Hua University, Hsinchu City, Taiwan, 2002.
51. Huang, P.-K. Research of Multi-Component High-Entropy Alloys for Thermalspray Coating. Master's Thesis, National Tsing Hua University, Hsinchu City, Taiwan, 2003.
52. Lin, Y.-F. Particle Erosion Characteristics of a Plasma-Sprayed Zr-Based High-Entropy Alloy. Bachelor's Thesis, National Cheng Kung University, Tainan City, Taiwan, 2004.
53. Lin, M.-S. Study on the Corrosion Behavior and Thin Film Properties of Cr-Fe-Co-Ni-Cu-Al_x High-Entropy Alloys. Master's Thesis, Chinese Culture University, Taipei City, Taiwan, 2003.

54. Hsu, Y.-J. Corrosion Behavior of FeCoNiCrCu High-Entropy Alloys in Various Aqueous Solutions. Master's Thesis, National Taiwan Ocean University, Keelung City, Taiwan, 2004.
55. Huang, C.-M. The Study of Different Welding With High-Entropy and SUS304 Stainless Steels. Master's Thesis, National Chiao Tung University, Hsinchu City, Taiwan, 2004.
56. Chung, S.-Y. Investigation of the Machinability of Five Kinds of High-Entropy Alloys and the Effects of Al, Cu, Co Elements Inclusion. Master's Thesis, National Taiwan University, Taipei City, Taiwan, 2004.
57. Chen, M.J. The Effect of V, Si, Ti Addition on the Microstructure and Wear Properties of Al(0.5)CrCuFeCoNi High-Entropy Alloys. Master's Thesis, National Tsing Hua University, Hsinchu City, Taiwan, 2003.
58. Wu, C.M. Research for the Adhesive Wear Properties of Al_xCoCuFeNiTi_y High-Entropy Alloys. Master's Thesis, National Tsing Hua University, Hsinchu City, Taiwan, 2004.
59. Huang, K.-H. A Study on the Multicomponent Alloy Systems Containing Equal-Mole Elements. Master's Thesis, National Tsing Hua University, Hsinchu City, Taiwan, 1996.
60. Lai, G.T. Properties of the Multicomponent Alloy System with Equal-Mole Elements. Master's Thesis, National Tsing Hua University, Hsinchu City, Taiwan, 1998.
61. Hsu, Y.-H. A Study on the Multicomponent Alloy Systems with Equal-Mole FCC or BCC Elements. Master's Thesis, National Tsing Hua University, Hsinchu City, Taiwan, 2000.
62. Hung, Y.-T. A Study on the Cu-Ni-Al-Co-Cr-Fe-Si-Ti Multicomponent Alloy System. Master's Thesis, National Tsing Hua University, Hsinchu City, Taiwan, 2001.
63. Bustamante, C.; Marko, J.; Siggia, E.; Smith, S. Entropic elasticity of lambda-phage DNA. *Science* **1994**, *265*, 1599–1600. [[CrossRef](#)] [[PubMed](#)]
64. Gardel, M.L.; Shin, J.H.; MacKintosh, F.C.; Mahadevan, L.; Matsudaira, P.; Weitz, D.A. Elastic behavior of cross-linked and bundled actin networks. *Science* **2004**, *304*, 1301–1305. [[CrossRef](#)] [[PubMed](#)]
65. Chaudhuri, O.; Parekh, S.H.; Fletcher, D.A. Reversible stress softening of actin networks. *Nature* **2007**, *445*, 295–298. [[CrossRef](#)] [[PubMed](#)]
66. Zhang, F.; Wu, Y.; Lou, H.B.; Zeng, Z.D.; Prakapenka, V.B.; Greenberg, E.; Ren, Y.; Yan, J.Y.; Okasinski, J.S.; Liu, X.J.; et al. Polymorphism in a high-entropy alloy. *Nat. Commun.* **2017**, *8*. [[CrossRef](#)] [[PubMed](#)]
67. Tracy, C.L.; Park, S.; Rittman, D.R.; Zinkle, S.J.; Bei, H.; Lang, M.; Ewing, R.C.; Mao, W.L. High pressure synthesis of a hexagonal close-packed phase of the high-entropy alloy CrMnFeCoNi. *Nat. Commun.* **2017**, *8*, 15634. [[CrossRef](#)]
68. Huang, E.W.; Lin, C.-M.; Jain, J.; Shieh, S.R.; Wang, C.-P.; Chuang, Y.-C.; Liao, Y.-F.; Zhang, D.-Z.; Huang, T.; Lam, T.-N.; et al. Irreversible phase transformation in a CoCrFeMnNi high entropy alloy under hydrostatic compression. *Mater. Today Commun.* **2018**, *14*, 10–14. [[CrossRef](#)]
69. Zhang, F.; Lou, H.; Song, C.; Chen, X.; Zeng, Z.; Yan, J.; Zhao, W.; Wu, Y.; Lu, Z.; Zeng, Q.S. Effects of non-hydrostaticity and grain size on the pressure-induced phase transition of the CoCrFeMnNi high-entropy alloy. *J. Appl. Phys.* **2018**, *124*, 115901. [[CrossRef](#)]
70. Wang, L.; Zhang, F.; Nie, Z.; Wang, F.; Wang, B.; Zhou, S.; Xue, Y.; Cheng, B.; Lou, H.; Chen, X.; et al. Abundant polymorphic transitions in the Al_{0.6}CoCrFeNi high-entropy alloy. *Mater. Today Phys.* **2019**, *8*, 1–9. [[CrossRef](#)]
71. Zhao, R.; Kim, Y.; Chester, S.A.; Sharma, P.; Zhao, X. Mechanics of hard-magnetic soft materials. *J. Mech. Phys. Solids* **2019**, *124*, 244–263. [[CrossRef](#)]
72. Zhang, Y.; Zhang, M.; Li, D.; Zuo, T.; Zhou, K.; Gao, M.; Sun, B.; Shen, T. Compositional design of soft magnetic high entropy alloys by minimizing magnetostriction coefficient in (Fe_{0.3}Co_{0.5}Ni_{0.2})_{100-x}(Al_{1/3}Si_{2/3})_x System. *Metals* **2019**, *9*, 382. [[CrossRef](#)]
73. Zhao, R.-F.; Ren, B.; Zhang, G.-P.; Liu, Z.-X.; Cai, B.; Zhang, J. CoCr_xCuFeMnNi high-entropy alloy powders with superior soft magnetic properties. *J. Magn. Magn. Mater.* **2019**, *491*, 165574. [[CrossRef](#)]
74. Koželj, P.; Vrtnik, S.; Jelen, A.; Krnel, M.; Gačnik, D.; Dražič, G.; Meden, A.; Wencka, M.; Jezeršek, D.; Leskovec, J.; et al. Discovery of a FeCoNiPdCu high-entropy alloy with excellent magnetic softness. *Adv. Eng. Mater.* **2019**, *21*, 1801055. [[CrossRef](#)]
75. Borkar, T.; Chaudhary, V.; Gwalani, B.; Choudhuri, D.; Mikler, C.V.; Soni, V.; Alam, T.; Ramanujan, R.V.; Banerjee, R. A combinatorial approach for assessing the magnetic properties of high entropy alloys: Role of Cr in AlCo_xCr_{1-x}FeNi. *Adv. Eng. Mater.* **2017**, *19*. [[CrossRef](#)]

76. Zuo, T.; Gao, M.C.; Ouyang, L.; Yang, X.; Cheng, Y.; Feng, R.; Chen, S.; Liaw, P.K.; Hawk, J.A.; Zhang, Y. Tailoring magnetic behavior of CoFeMnNiX (X = Al, Cr, Ga, and Sn) high entropy alloys by metal doping. *Acta Mater.* **2017**, *130*, 10–18. [[CrossRef](#)]
77. Li, P.; Wang, A.; Liu, C.T. Composition dependence of structure, physical and mechanical properties of FeCoNi(MnAl) x high entropy alloys. *Intermetallics* **2017**, *87*, 21–26. [[CrossRef](#)]
78. Feng, W.; Qi, Y.; Wang, S. Effects of short-range order on the magnetic and mechanical properties of FeCoNi(AlSi)x high entropy alloys. *Metals* **2017**, *7*, 482. [[CrossRef](#)]
79. Ma, S.G.; Jiao, Z.M.; Qiao, J.W.; Yang, H.J.; Zhang, Y.; Wang, Z.H. Strain rate effects on the dynamic mechanical properties of the AlCrCuFeNi2 high-entropy alloy. *Mater. Sci. Eng. A* **2016**, *649*, 35–38. [[CrossRef](#)]
80. Jin, P.; Ye, P.; Hui, Z.; Lu, Z. Microstructure and properties of AlCrFeCuNix (0.6 ≤ x ≤ 1.4) high-entropy alloys. *Mater. Sci. Eng. A* **2012**, *534*, 228–233. [[CrossRef](#)]
81. Liu, L.; Zhu, J.B.; Li, J.C.; Jiang, Q. Microstructure and magnetic properties of FeNiCuMnTiSnx High entropy alloys. *Adv. Eng. Mater.* **2012**, *14*, 919–922. [[CrossRef](#)]
82. Davis, J.R. *Metals Handbook, DESK EDITION*, 2nd ed.; ASM International: Materials Park, OH, USA, 2003.
83. Diez-Jimenez, E.; Rizzo, R.; Gómez-García, M.-J.; Corral-Abad, E. Review of passive electromagnetic devices for vibration damping and isolation. *Shock Vib.* **2019**, *2019*, 16. [[CrossRef](#)]
84. Aranke, O.; Algenaid, W.; Awe, S.; Joshi, S. Coatings for automotive gray cast iron brake discs: A review. *Coatings* **2019**, *9*, 552. [[CrossRef](#)]
85. Trout, S. Material selection of permanent magnets, considering thermal properties correctly. In Proceedings of the Electrical Insulation Conference and Electrical Manufacturing and Coil Winding Conference (Cat. No.01CH37264), Cincinnati, OH, USA, 18 October 2001; pp. 365–370. [[CrossRef](#)]
86. Fu, Z.; MacDonald, B.E.; Dupuy, A.D.; Wang, X.; Monson, T.C.; Delaney, R.E.; Pearce, C.J.; Hu, K.; Jiang, Z.; Zhou, Y.; et al. Exceptional combination of soft magnetic and mechanical properties in a heterostructured high-entropy composite. *Appl. Mater. Today* **2019**, *15*, 590–598. [[CrossRef](#)]
87. Firstov, G.S.; Kosorukova, T.A.; Koval, Y.N.; Odnosum, V.V. High entropy shape memory alloys. *Mater. Today Proc.* **2015**, *2*, S499–S503. [[CrossRef](#)]
88. Ma, L.; Wang, L.; Nie, Z.; Wang, F.; Xue, Y.; Zhou, J.; Cao, T.; Wang, Y.; Ren, Y. Reversible deformation-induced martensitic transformation in Al0.6CoCrFeNi high-entropy alloy investigated by in situ synchrotron-based high-energy X-ray diffraction. *Acta Mater.* **2017**, *128*, 12–21. [[CrossRef](#)]
89. Fan, Z.; Wang, H.; Wu, Y.; Liu, X.J.; Lu, Z.P. Thermoelectric high-entropy alloys with low lattice thermal conductivity. *RSC Adv.* **2016**, *6*, 52164–52170. [[CrossRef](#)]
90. Herzog, D.; Seyda, V.; Wycisk, E.; Emmelmann, C. Additive manufacturing of metals. *Acta Mater.* **2016**, *117*, 371–392. [[CrossRef](#)]
91. Starr, T.; Rafi, H.; Stucker, B.; Scherzer, C.M. *Controlling Phase Composition in Selective Laser Melted Stainless Steels*; University of Louisville: Louisville, KY, USA, 2012; pp. 439–446.
92. Tsai, P.-I.; Lam, T.-N.; Wu, M.-H.; Tseng, K.-Y.; Chang, Y.-W.; Sun, J.-S.; Li, Y.-Y.; Lee, M.-H.; Chen, S.-Y.; Chang, C.-K. Multi-scale mapping for collagen-regulated mineralization in bone remodeling of additive manufacturing porous implants. *Mater. Chem. Phys.* **2019**, *230*, 83–92. [[CrossRef](#)]
93. Huang, E.-W.; Lee, S.Y.; Jain, J.; Tong, Y.; An, K.; Tsou, N.-T.; Lam, T.-N.; Yu, D.; Chae, H.; Chen, S.-W. Hardening steels by the generation of transient phase using additive manufacturing. *Intermetallics* **2019**, *109*, 60–67. [[CrossRef](#)]
94. Hong, H.H.; Hong, A.; Wang, C.C.; Huang, E.W.; Chiang, C.C.; Yen, T.H.; Huang, Y.F. Calcitriol exerts a mineralization-inductive effect comparable to that of vitamin C in cultured human periodontium cells. *Am. J. Transl. Res.* **2019**, *11*, 2304–2316. [[PubMed](#)]
95. Hadush Tesfay, A.; Chou, Y.-J.; Tan, C.-Y.; Fufa Bakare, F.; Tsou, N.-T.; Huang, E.-W.; Shih, S.-J. Control of dopant distribution in yttrium-doped bioactive glass for selective internal radiotherapy applications using spray pyrolysis. *Materials* **2019**, *12*, 986. [[CrossRef](#)] [[PubMed](#)]
96. Chae, H.; Huang, E.W.; Jain, J.; Wang, H.; Woo, W.; Chen, S.-W.; Harjo, S.; Kawasaki, T.; Lee, S.Y. Plastic anisotropy and deformation-induced phase transformation of additive manufactured stainless steel. *Mater. Sci. Eng. A* **2019**, *762*, 138065. [[CrossRef](#)]
97. Zhu, Z.G.; Nguyen, Q.B.; Ng, F.L.; An, X.H.; Liao, X.Z.; Liaw, P.K.; Nai, S.M.L.; Wei, J. Hierarchical microstructure and strengthening mechanisms of a CoCrFeNiMn high entropy alloy additively manufactured by selective laser melting. *Scr. Mater.* **2018**, *154*, 20–24. [[CrossRef](#)]

98. Zhu, Z.G.; Ng, F.L.; Qiao, J.W.; Liaw, P.K.; Chen, H.C.; Nai, S.M.L.; Wei, J.; Bi, G.J. Interplay between microstructure and deformation behavior of a laser-welded CoCrFeNi high entropy alloy. *Mater. Res. Express* **2019**, *6*, 046514. [[CrossRef](#)]
99. Chen, S.; Tong, Y.; Liaw, P.K. Additive manufacturing of high-entropy alloys: A review. *Entropy* **2018**, *20*, 937. [[CrossRef](#)]
100. Zhou, R.; Liu, Y.; Zhou, C.; Li, S.; Wu, W.; Song, M.; Liu, B.; Liang, X.; Liaw, P.K. Microstructures and mechanical properties of C-containing FeCoCrNi high-entropy alloy fabricated by selective laser melting. *Intermetallics* **2018**, *94*, 165–171. [[CrossRef](#)]



© 2020 by the authors. Licensee MDPI, Basel, Switzerland. This article is an open access article distributed under the terms and conditions of the Creative Commons Attribution (CC BY) license (<http://creativecommons.org/licenses/by/4.0/>).